J Solid State Electrochem (2012) 16:2227–2233
DOI 10.1007/s10008-012-1655-1

ORIGINAL PAPER

Success and serendipity on achieving high energy density for rechargeable batteries

Manickam Minakshi · Pritam Singh

Received: 30 November 2011 / Revised: 5 January 2012 / Accepted: 10 January 2012 / Published online: 26 January 2012

Abstract Rechargeable lithium batteries that use non-aqueous electrolytes may not be suitable for electric vehicle applications, which require safe, inexpensive, and high energy density. In this paper, we showed that reversible lithium intercalation can occur in MnO_2 cathode coupled with Zn anode while using LiOH aqueous electrolyte. This new Zn|LiOH|MnO_2 aqueous rechargeable cell could operate around 1.5 V for multiple cycles and possibly be used in battery packs, are of low cost, and environmentally benign. However, higher energy density, power density, and cycling life of the Zn|LiOH|MnO_2 system are required for exploiting this technology to better compete with the lithium battery counterparts. Serendipitously, high energy density (270 Wh/Kg) that was achieved with physically mixed additives (Bi_2O_3 and TiB_2) on MnO_2 is reported. Physically modified cathode containing multiple additives is shown to be superior in energy density and capacity retention compared to that of the additive-free MnO_2 or carbon-coated MnO_2 using polyvinylpyrrolidone as the source. The role of the additives (Bi_2O_3 and Bi_2O_3+TiB_2) in the MnO_2 electrode is found to avoid the formation of unwanted (non-rechargeable) products and to decrease the polarization of the electrode.

Keywords MnO_2 · Serendipity · Additives · Capacity · Aqueous battery

M. Minakshi (✉) · P. Singh
Faculty of Minerals and Energy, Murdoch University,
Murdoch, WA 6150, Australia
e-mail: minakshi@murdoch.edu.au

M. Minakshi
e-mail: lithiumbattery@hotmail.com

Introduction

Today, nickel–metal hydride (Ni-MH) technology is the principal battery used in hybrid electric vehicles [1, 2] but it can be displaced by the higher-energy lithium-ion technology if the latter's lifetime, high cost of manufacture, and safety issues can be sizeably tailored. Although numerous progresses have been achieved in the development of lithium-ion technology both in terms of electrode materials and of electrolytes, problems posed on capacity fading upon cycling due to the formation of solid-electrolyte interphase by electrolyte degradation still remain [3, 4]. This implies a decrease in the lifetime of the batteries. Alternate cathodes and electrolytes for Li-ion technologies are being investigated for high energy density, safer, and cheaper batteries worldwide [5–9] but improvements in safety have in general further lowered battery capacity. Researchers at Murdoch University have been conducting research into an alternative secondary battery system based upon the existing alkaline Zn/MnO_2 primary system [10–12]. This new aqueous rechargeable battery technology developed successfully by the author (M. Minakshi) at Murdoch University is low cost, environmentally friendly, and inherently safe. This rechargeable battery chemistry appears to meet the energy and power demands of household consumer devices and their characteristics are compared in Table 1 with other types of batteries currently used in hybrid electric vehicles.

Among promising candidates for cathode materials in aqueous batteries, manganese-dioxide-based systems have been extensively investigated due to their attractive characteristics that include low cost, low toxic, available in plenty, and safe to handle [13, 14]. Manganese dioxide (MnO_2) is recognized as a potentially high energy cathode, but long-term attempts to develop this alkaline primary system into a rechargeable battery has failed [15, 16]. Existing non-

Table 1 Battery types currently used in hybrid electric vehicles and their common characteristics compared with Zn|LiOH|MnO_2 aqueous rechargeable battery [35]

Battery types	Energy density (Wh/kg)	Power density (W/kg)	Safety	Current cost ($/kWh)
Lead acid	25–35	75–130	Environmentally not good otherwise OK	100 to 125
Nickel–metal hydride	50–80	150–250	Not safe	525 to 540
Lithium ion ($LiFePO_4$)	80–100	375–475	Not safe	About 1,000
Zn|LiOH|MnO_2	270	65–75	Safe	100 to 125

rechargeable alkaline Zn/MnO_2 batteries use an aqueous KOH electrolyte [15, 17]. These cells are based on the insertion of protons (H^+) into MnO_2, a non-reversible process. It was widely believed that all aqueous electrolytic systems similarly resulted in only proton insertion. However, our work at Murdoch based on an aqueous lithium hydroxide (LiOH) electrolyte has succeeded in showing that it can result in the insertion of lithium ions into MnO_2 [18]. This battery has been tested in the lab and has demonstrated the potential to lead to a new field of rechargeable alkaline batteries. Improvements to energy density are not only possible through the use of MnO_2, but furthermore as lithium aqueous electrolytes have ion conductivities about two orders of magnitude higher than their non-aqueous counterparts [19].

Bottlenecks in developing this technology include improving the suppression of unwanted discharge products to improve the rate capability and energy density of this battery. Additives such as bismuth oxide (Bi_2O_3) or titanium disulphide (TiS_2) incorporated into the cathode [20, 21] have resulted in improvements and another set of additives (alkaline earth oxides, i.e., BaO, MgO, and CaO) [22] trialed have resulted in further improved recharge capacity and cycle performance. The set of additives based on alkaline earth oxides resulted in a patent cooperation treaty application [23].

In aqueous rechargeable battery system, during the cell discharge, mechanism involves both lithium and proton intercalation into the host MnO_2 compound [20, 21]. The intake of proton insertion resulted in manganese oxy hydroxide (MnOOH) as the discharged product [15]. The MnOOH in the electrode undergoes a dissolution reaction that releases Mn^{3+} ions into the electrolyte [24]. The Mn^{3+} species are further reduced to a soluble Mn^{2+} that subsequently precipitates to form the end products such as Mn_2O_3 and $Mn(OH)_2$. Interestingly, our preliminary studies [20–22] showed that the incorporation of additives such as CeO_2, MgO, TiS_2, or Bi_2O_3 compounds in a suitable proportion into the MnO_2 cathode retard this disproportionation reaction of Mn^{3+} by keeping the Mn^{3+} ions in the solution for a longer time, i.e., during the discharge process and thereby prevent the formation of unwanted non-rechargeable products like Mn_2O_3, $Mn(OH)_2$, and Mn_3O_4. This mechanism is quite similar to that proposed by Manthiram et al. [25]. This leads to improved energy density in the MnO_2 cathode. These fundamental studies on incorporating additives in Zn-MnO_2 aqueous rechargeable system will offer, for the first time, a database of knowledge that can be used by battery technologists in identifying suitable materials for designing new positive electrodes for an aqueous rechargeable battery. The key concept and strategy lies in transforming the primary (non-rechargeable) battery into a high-performance secondary (rechargeable) battery while using aqueous lithium hydroxide as an electrolyte with Zn as the negative electrode.

In this study, two approaches have been pursued to render higher energy density to Zn-MnO_2 rechargeable battery. One approach is we have tried a unique synthetic method to carbon coat the MnO_2 particles using polyvinylpyrrolidone (PVP) as a source. This enhances the conductivity and lithium intercalation mechanism during discharge but reduces the working voltage of MnO_2 cathode. The second approach is the incorporation of small amounts of TiB_2 additive through physical mixing that found to enhance the capacity without any decrement of voltage. On the other hand, the extension of second approach to multiple additives consisting TiB_2 and Bi_2O_3 further improves the capacity (energy density) and cycling life. In this paper, we have reported the synthetic method and potential additives could make the rechargeable alkaline batteries suitable for vehicular applications.

Experimental

The electrolytic manganese dioxide of γ-MnO_2 type (IBA sample 32) material used in this work was purchased from the Kerr McGee Chemical Corporation. Bismuth oxide (Bi_2O_3), polyvinylpyrrolidone was obtained from Aldrich chemical company and titanium diboride (TiB_2) from Alfa Aesar. For PVP-assisted MnO_2, metal oxide powder (MnO_2) was dissolved in water at 80 °C with an effective stirring to obtain a homogenous solution. Then the PVP was added in 1:1 weight ratio to the metal ions. The process of stirring and heating was continued until thick transparent gel was obtained. Then, the gel was dried at 110 °C in hot oven

for 10 h. Finally, the product was heated at 275 °C for 3 h in air to get the PVP decomposed.

For cyclic voltammetric (CV) experiments, a standard three-electrode cell was used. For this purpose, the γ-MnO_2 working electrode was made as follows: γ-MnO_2 powder (with 0 and 5 wt.% of additives (TiB_2, or Bi_2O_3 + TiB_2)) or PVP-assisted MnO_2 powder was pressed on to a disk of Pt gauze. On the other side of a disk, a layer of conductive carbon (A-99, Asbury USA) was also pressed. The MnO_2 side of the disk was exposed to the LiOH electrolyte through a Teflon barrel. The schematic diagram is shown in Fig. 1. For making electrical connection of MnO_2 a Pt disk was inserted into the barrel on top of the carbon side which contacted a stainless steel plunger. The counter electrode was a zinc foil, which was separated from the main electrolyte by means of a porous frit. A mercury–mercuric oxide (Hg/HgO) served as the reference electrode. The standard concentration of the electrode filling solution is 4.2 M KOH. Reported potentials are relative to Hg/HgO. The electrolyte used for battery experiments was a saturated amount of aqueous lithium hydroxide. The working electrode was cycled between 0.2 and −0.45 V at a slow-scan rate of 25 μV s^{-1} scan rate. On each occasion the potential scan started at 0.2 V, moving initially in the cathodic direction and then reversed back anodically to the starting point.

For battery (galvanostatic) experiments, a Swagelok-type two-cell electrode was used. The γ-MnO_2 active material was first mixed with ((0 and 5 wt.% of suitable additives (TiB_2, or Bi_2O_3 + TiB_2) or PVP-assisted MnO_2 powder)), along with 15 wt.% of carbon black and 10 wt.% of poly (vinylidene difluoride) (PVDF, Sigma Aldrich) as a binder and then pressed into a disk shape with a diameter of 12 mm. Each disk was 0.3 mm thick and the active mass weighed approximately 25 mg. An electrochemical test cell was constructed with the disk as the cathode, Zn metal as the anode, and filter paper (Whatman filters 12) as the separator. The cell was discharged/charged galvanostatically using an eight channel battery analyzer from Neware, China, operated by a battery testing system. The cut-off discharge and charge voltages were 1.0 and 1.9 V, respectively. All electrochemical measurements were carried out at ambient temperature. For all experiments, a constant charge/discharge current of 0.2 mA on mass density (8 mA/g) was used.

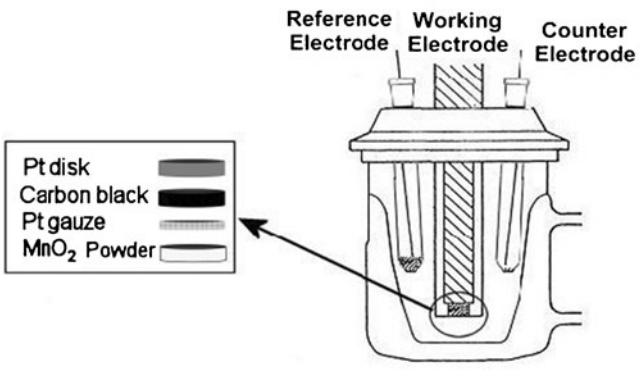

Fig. 1 Schematic diagram of a potentiostatic (three-cell) configuration [36]

Results and discussion

Figure 2 shows a typical slow-scan cyclic voltammetric behavior of MnO_2 in aqueous LiOH electrolyte. The scan was initiated at 200 mV going in the cathodic direction to −350 mV and then reversing it to the starting potential. During the first cathodic sweep, a reduction peak C_1 is seen at a potential −280 mV. During the reverse anodic sweep, an oxidation peak A_1 is seen at −69 mV. Thus the material MnO_2 undergoes electro-reduction/oxidation corresponding to lithium (Li_xMnO_2) [10] and proton (δ-MnOOH) [26] insertion during reduction and extraction of lithium ($Li_{1-x}MnO_2$) during oxidation of Mn atom in MnO_2. On repeated cycling, the position of the reduction peak C_1 shifted more negatively (−315 mV), changed in current intensity and its shape while comparing to that of the first cycle. These observations suggest that the electro-reduction processes of MnO_2 on repeated cycling is not fully reversible. However, the oxidation peak (A_1) position was not altered. A shoulder of anodic peak (A_2 at 30 mV) is also seen corresponding to δ-MnOOH. The γ-MnO_2 (an inter growth of pyrolusite and ramsdellite) after electro-reduction becomes δ-MnOOH by the intercalation of protons into the tunnels and the un-reacted amount of δ-MnOOH is seen during the anodic scan [26]. A typical galvanostatic (discharge–charge) curve of the Zn-MnO_2 aqueous LiOH cell is shown in Fig. 3. The initial open-circuit voltage (OCV) was 1.8 V. On discharge at a current of 0.2 mA the cell voltage dropped slightly lower to 1.65 V and then had a plateau-like

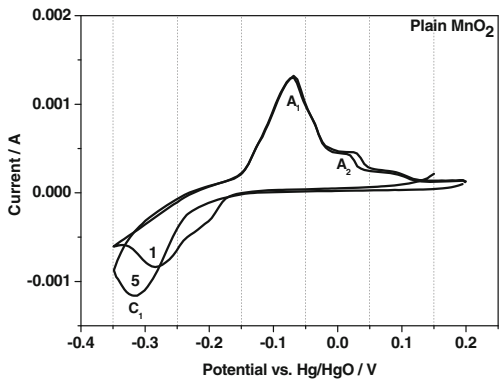

Fig. 2 Cyclic voltammogram for plain MnO_2 electrode (0 wt.% additive) in saturated LiOH electrolyte. Voltage was swept cathodically initially from +0.2 V to −0.35 V and back at a scan rate of 25 μV s^{-1}. Cycle numbers are indicated in the figure

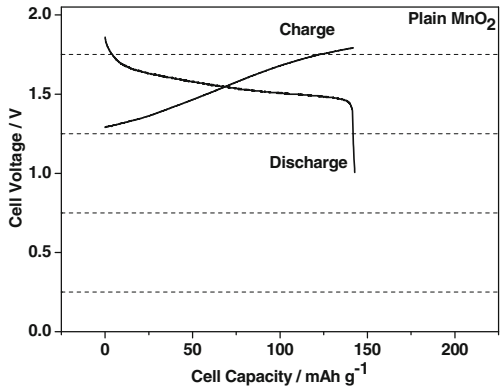

Fig. 3 Constant current discharge–charge curves of plain MnO_2 (0 wt. % additive) cathode in Zn|LiOH|MnO_2 battery

curve at 1.55 V corresponding to $Mn^{4+/3+}$ redox couple before it fell down to 1.0 V. The cell discharge capacity was calculated to be about 140 mAh g^{-1}. As can be seen from Fig. 2, the cell could be fully charged back to 1.8 V with a 100% material utilization back to parent MnO_2. Figure 4 shows the cyclability of the MnO_2 cathode material in the presence and absence of additives. After multiple cycling, at the 25th cycle, the available capacity for MnO_2 (0 wt.% additive) was found to be just 100 mAh g^{-1} (30% loss in Fig. 4 (a)) suggesting that the material was degrading to a larger extent.

To enhance the cyclability of the MnO_2 aqueous rechargeable system, unique polymer-assisted synthetic method is chosen to coat the MnO_2 active material. A polymer, i.e., polyvinylpyrrolidone is added to the MnO_2 colloid dispersion as explained in the Experimental section. In solution, PVP is soluble and has excellent wetting properties, thus making it as a good candidate for carbon coating on the surface of MnO_2 cathode [27]. PVP contains nitrogen and oxygen atoms in their molecular structure. The nitrogen dioxide interaction with polymers containing imide groups in the main chains of PVP establishes strong affinity to a single unit of MnO_2 colloid. This imide and metal bonding stabilize the particle size and prevent particle aggregation that is the characteristic of PVP [28]. Finally, heating the MnO_2 containing PVP mixture melts the PVP and decomposes. The decomposed product was a unique carbon-coated [29] manganese dioxide. Figure 5 shows a typical cyclic voltammetric behavior of PVP-assisted MnO_2 used in this study. During the first cycle, one reduction (C_1) and one oxidation peak (A_1) at −310 and −88 mV, respectively, are seen. On repeated cycling, two reduction peaks C_1 and C_2, at potentials −340 and −265 mV, respectively, are seen. However, on the reverse anodic sweep only one peak A_1 at −50 mV was observed. The well resolved reduction peaks C_1 and C_2 corresponds to lithium and proton insertion respectively. The polymer layer is active only after an initial oxidation and hence the appearance of peak C_2 from the second cycle onwards. The absence of peak A_2 (in Fig. 5) indicates the system is fully reversible with the aid of PVP-added MnO_2. The coated PVP on the MnO_2 layer facilitate the reduction reaction mechanism leading to an increase in discharge capacity and well-defined redox peaks. Although the motivation is achieved, in terms of multiple cycling and efficiency of the battery, the area under the peaks is still marginal and may not be suffice for vehicular applications as energy density is a pre-requisite. This is further supported by the discharge–charge behavior of the Zn-PVP-added MnO_2 battery. A typical behavior of the aqueous cell is shown in Fig. 6. The initial OCV was 1.5 V, which is 0.3 V lower than the plain MnO_2 (containing no additive). The flat discharge voltage of this battery is around 1.2 V, comprising a total discharge capacity of 200 mAh g^{-1}. The carbon-coated MnO_2 material enhanced the battery storage capacity to 30% but the synthetic manipulations (MnO_2

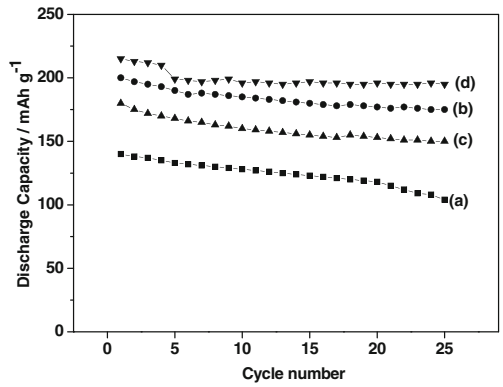

Fig. 4 Cyclability of Zn|LiOH|MnO_2 battery in the presence and absence of additives. MnO_2 cathode containing (*a*) 0 wt.%, (*b*) PVP, (*c*) 5 wt.% TiB_2, and (*d*) 3 wt.% TiB_2 + 2 wt.% Bi_2O_3 additives

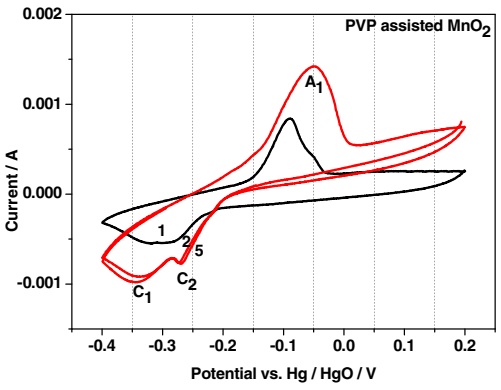

Fig. 5 Cyclic voltammogram for PVP-assisted MnO_2 electrode in saturated LiOH electrolyte. Voltage was swept cathodically initially from +0.2 V to −0.45 V and back at a scan rate of 25 μV s^{-1}. Cycle numbers are indicated in the figure

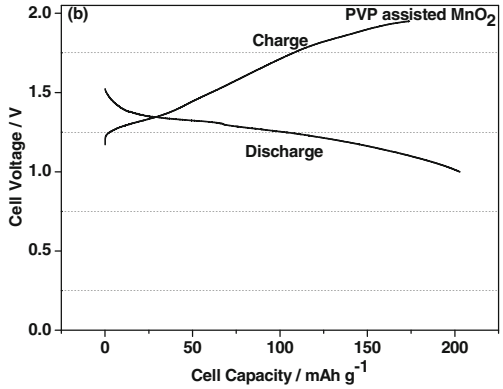

Fig. 6 Constant current discharge–charge curves of PVP-assisted MnO_2 cathode in Zn|LiOH|MnO_2 battery

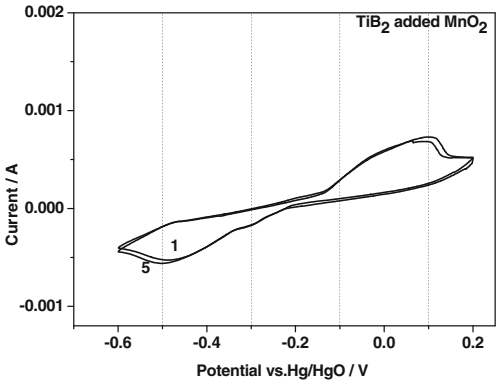

Fig. 7 Cyclic voltammogram for TiB_2 (5 wt.%) added MnO_2 electrode in saturated LiOH electrolyte. Voltage was swept cathodically initially from +0.2 V to −0.6 V and back at a scan rate of 25 μV s^{-1}. Cycle numbers are indicated in the figure

colloidal dispersions with PVP and further heating) decreased the open-circuit voltage of the raw MnO_2 material to 0.3 V and hence the shape in the discharge curve. The lower discharge voltage of 1.2 V is a drawback for PVP as a source which may be difficult to compete with the current battery benchmark. Although a large capacity loss (as what observed for plain MnO_2) is not seen in the multiple cycles (Fig. 4 (b)), but a steady fade is found to continue and at the end of 25th cycle the discharge capacity was found to be 175 mAh g^{-1}, loss of 13% efficiency.

As detailed in the Introduction section, small amount of an incorporation of additives through physical mixing in the MnO_2 cathode provided an important advantage in terms of energy density. An early development in this approach was initiated at the Ford Motor Company [30, 31]. Subsequent to this, several other researchers [15, 16, 24, 25] have focused on additives in the MnO_2 cathode material but all their work was mainly restricted to primary batteries. Our group showed a range of additives as listed in the Introduction section for aqueous secondary batteries. Here, in this study we have used titanium diboride (TiB_2) and bismuth oxide (Bi_2O_3) as an additive source in MnO_2 active material. Addition of a small amount of TiB_2 (3 wt.%) physically mixed into MnO_2 produces a typical cyclic voltammetric and galvanostatic behavior as shown in Figs. 7 and 8. The redox behavior seen from the CV (Fig. 7) illustrates one reduction (C_1) and oxidation peak (A_1) at −490 and 100 mV, respectively. The wide potential between the reduction and oxidation potentials is because of the high overpotential of the reduction/oxidation reactions. This is not surprising given the similar potential difference seen through the discharge–charge curve in Fig. 8. A very similar electrochemical performance is also observed by Manthiram et al. [25] for the TiB_2 additive. The area under the curve is significantly lowered than the polymer-added MnO_2, however, due to the presence of titanium (an excellent conductor of electricity [32]) that enhanced the voltage profile and the storage capacity. The observed shift in the reduction peaks may be due to the changes in the nature of electro-reduced material formed during the reduction process in the presence of TiB_2 as an additive. The cell is found to be fully reversible with a capacity of 180 mAh g^{-1}. After 25 cycles, the discharge capacity was lowered to 150 mAh g^{-1}, with a loss of 17% efficiency as seen in Fig. 4 (c).

With an objective of understanding the role of bismuth (Bi_2O_3) as additive in the presence of TiB_2, the following experiment was performed. The MnO_2 active material was physically mixed with multiple additives (Bi_2O_3 2 wt.% + TiB_2 3 wt.%) and subjected to redox reactions and discharge–charge processes. The choice of Bi_2O_3 stems from the fact that bismuth acts as a pillaring effect in stabilizing the host MnO_2 structure [33] and to reduce the activation energy (overpotential) of the charge and discharge processes involving Mn^{3+} [34]. The combination of these two additives is more likely to provide the multiple services required

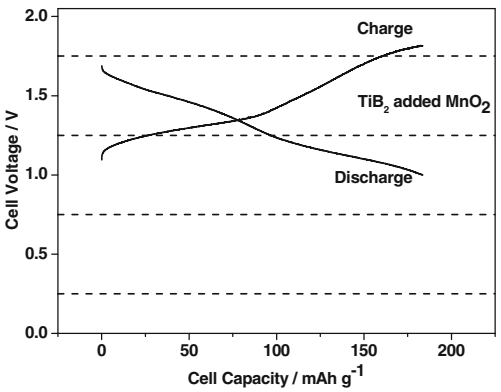

Fig. 8 Constant current discharge–charge curves of TiB_2 (5 wt.%) added MnO_2 cathode in Zn|LiOH|MnO_2 battery

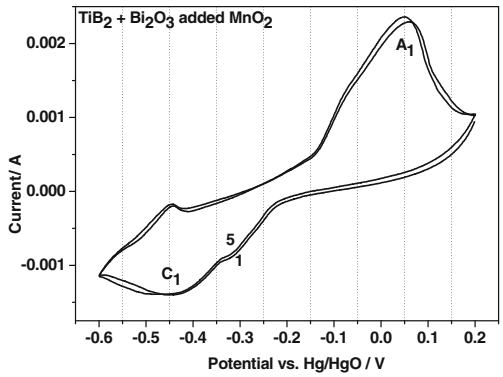

Fig. 9 Cyclic voltammogram for TiB_2 (3 wt.%) + Bi_2O_3 (2 wt.%) added MnO_2 electrode in saturated LiOH electrolyte. Voltage was swept cathodically initially from +0.2 V to −0.6 V and back at a scan rate of 25 μV s^{-1}. Cycle numbers are indicated in the figure

for higher energy density. The CV profile of the multiple additives (in Fig. 9) consists of a well-defined reduction peak at C_1 −450 mV and a corresponding anodic peak A_1 at 50 mV. The ratio of the charge under the peaks C_1 and A_1 was 90% reversible. The presence of these multiple additives suggests to block/delay the dissolution of Mn^{3+} ions thereby inhibiting the formation of unwanted rechargeable products (like MnOOH, $Mn(OH)_2$ or δ-MnOOH) during reduction. In other words, redox couple $Mn^{4+/3+}$ stays longer when bismuth and titanium diboride additives are present and hence the capacity. Serendipitously, the effect of Bi_2O_3 in the presence of TiB_2 is more effective than the carbon-coated MnO_2 using PVP as a source or TiB_2 by itself. The success of this multiple additive is also seen through discharge–charge cycle experiment in Fig. 10. The mid-discharge voltage and the available discharge capacity are competitive providing 1.25 V and 215 mAh g^{-1}, respectively. After 25 cycles, the discharge capacity was just lowered only to 195 mAh g^{-1}, with a loss of 10% efficiency as displayed in Fig. 4 (d). The

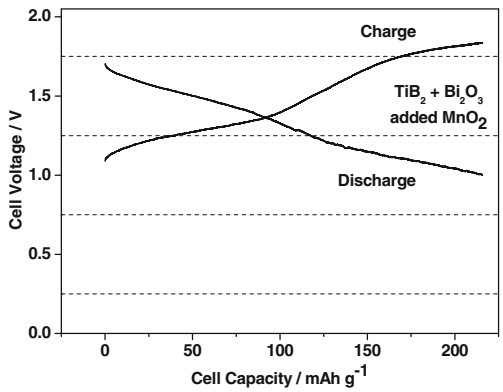

Fig. 10 Constant current discharge–charge curves of TiB_2 (3 wt.%) + Bi_2O_3 (2 wt.%) added MnO_2 cathode in Zn|LiOH|MnO_2 battery

battery with multiple additives is fully rechargeable while suppressing the non-rechargeable products, possessing excellent efficiency and minimal capacity fading. The aqueous rechargeable (Zn|LiOH|MnO_2) cell in the presence of mixed additives is characterized by an enhanced rechargeability with good capacity retention (as seen in Fig. 4) and coulombic efficiency (discharge/charge time ratio) even at 100% depth of discharge at C/5 rate. This will lead to the development low cost and low toxicity battery materials for potential applications in electric vehicles or household devices. Nevertheless, the Zn|LiOH|MnO_2 cell operating just above 1 V may restrict its application as a single module, but it could have advantages in battery packs that will enhance the power and find a market niche. An extensive cycling test using different C rates at various depth of discharge is required to warrant for commercial application

Conclusions

The objective to identify "eco-benign" and economically viable cathode materials that can be used in aqueous rechargeable batteries has been achieved successfully with high energy density. The behavior of MnO_2 in aqueous LiOH illustrated that both the lithium and proton are intercalated into the MnO_2 and the electrochemical process is not fully reversible. The discharge capacity of 140 mAh g^{-1} to 1 V cut-off voltage could be achieved and there was a quick fade in capacity, losing up to 30% efficiency after 25th cycle. The carbon-coated MnO_2 (with unique polymer as a source) enhanced the conductivity and lithium intercalation mechanism leading to a well-resolved reduction peaks C_1 and C_2 with a discharge capacity of 200 mAh g^1 and the capacity fade is minimized to 13%. However, the working voltage was low (1.2 V) as the raw MnO_2 material was altered during colloidal dispersion and not readily suitable for potential applications. The addition of small amounts of TiB_2 was found to improve the open-circuit voltage but the rechargeability and working voltage was not up to the benchmark. Whereas, serendipitously, the presence of Bi_2O_3 in TiB_2 (multiple additives) performed well providing a good storage capacity (215 mAh g^{-1} or 270 Wh/Kg) and capacity retention (to 10% loss). The presence of these multiple additives suppresses the formation of non-rechargeable products while enhancing the lithium insertion into MnO_2 structure. Bi_2O_3+TiB_2 additives are more effective than PVP-assisted MnO_2.

Acknowledgments The author Minakshi wishes to acknowledge the Australian Research Council and Centre for Research into Energy for Sustainable Transport (CREST). This research was supported under Australian Research Council's Discovery Projects funding scheme (DP1092543) and CREST (Center of Excellence, Project 1.1.5).

References

1. Fetcenko MA, Ovshinsky SR, Reichman B, Young K, Fierro C, Koch J, Zallen A, Mays W, Ouchi T (2007) J Power Sources 165:544–551
2. Ramesh TN, Kamath PV (2008) J Power Sources 175:625–629
3. Nguyen CC, Song SW (2010) Electrochim Acta 55:3026–3033
4. Zhang Y, Wang CY, Tang X (2011) J Power Sources 196:1513–1520
5. Wright RB, Christophersen JP, Motloch CG, Belt JR, Ho CD, Battaglia VS, Barnes JA, Duong TQ, Sutula RA (2003) J Power Sources 119:865–869
6. Choi SS, Lim HS (2002) J Power Sources 111:130–136
7. Wu Q, Lu W, Prakash J (2000) J Power Sources 88:237–242
8. Li J, Murphy E, Winnick J, Kohl PA (2001) J Power Sources 102:294–301
9. Nagasubramanian G, Orendorff CJ (2011) J Power Sources 196:8604–8609
10. Minakshi M, Singh P, Issa TB, Thurgate S, De Marco R (2004) J Power Sources 130:254–259
11. Minakshi M, Pandey A, Blackford M, Ionescu M (2010) Energy Fuel 24:6193–6197
12. Minakshi M (2010) Electrochem Solid State Lett 9:A125–A127
13. Roberts AJ, Slade RCT (2010) Electrochim Acta 55:7460–7469
14. Spicak P, Sedlarikova M, Zatloukal M, Novak V, Kazelle J, Vondrak J, Jirak T (2009) J Solid State Electrochem 15:635–639
15. Kordesch K, Gsellmann J, Peri M, Tomantschger K, Chemelli R (1981) Electrochim Acta 26:1495–1504
16. Sajdl B, Micka K, Krtil P (1995) Electrochim Acta 40:2005–2011
17. Era A, Takehara Z, Yoshizawa S (1967) Electrochim Acta 12: 1199–1212
18. Minakshi M, Singh P, Carter M, Prince K (2008) Electrochem Solid State Lett 11:A145–A149
19. Li W, Dahn JR (1995) J Electrochem Soc 142:1742–1746
20. Minakshi M, Singh P, Mitchell DRG (2007) J Electrochem Soc 154:A109–A113
21. Minakshi M (2009) J Solid State Electrochem 13:1209–1214
22. Minakshi M, Blackford M, Ionescu M (2011) J Alloys Compd 509:5974–5980
23. Minakshi M (2011) Rechargeable battery. PCT (WO/2011/ 044644)
24. Im D, Manthiram A, Coffey B (2003) J Electrochem Soc 150: A1651–A1659
25. Rahuveer V, Manthiram A (2006) J Power Sources 163:598–603
26. Tye FL (1985) Electrochim Acta 30:17–23
27. Lee JM, Jun YD, Kim DW, Lee YH, Oh SG (2009) Mat Chem Phy 114:549–555
28. Bonet F, Delmas V, Grugeon S, Urbina RH, Silvert PY, Elhissen KT (1999) Nanostruct Mater 11:277–1284
29. Lee JS, Kwon OS, Park SJ, Park EY, You SA, Yoon H, Jang J (2011) ACS Nano 5:7992–8001
30. Wroblowa HS, Gupta N (1987) J Electroanal Chem 238:93–102
31. Yao YF, Gupta N, Wroblowa HS (1987) J Electroanal Chem 238:107–117
32. Schultes G, Schmitt M, Goettel D (2006) Freitag Weber O. Sens Actuators A Phys 126:287–291
33. Bach S, Pereiraramos JP, Baffier N, Messina R (1991) Electrochim Acta 36:595–1603
34. Qu D, Diehl D, Conway BE, Pell WG, Qian SY (2005) J Appl Electrochem 35:1111–1120
35. Battery Types and Characteristics for HEV, ThermoAnalytics, Inc (2007) http://www.thermoanalytics.com Accessed 04 Jan 2012
36. Minakshi M (2006) Thesis (PhD) Electrochemistry of cathode materials in aqueous lithium hydroxide electrolyte. Murdoch University, Australia